Recent Practical Applications of Radiative Transfer in Satellite Remote Sensing

P. Minnis, L. Nguyen, W. L. Smith, J. Murray

LaRC, Hampton, VA

K. Ayers, C. Yost, M. Khaiyer, R. Palikonda, D. Spangenberg

SSAI, Hampton, VA

F.-L. Chang

NIA, Hampton, VA

2007 AGU Fall Meeting

12 December 2007

Background

- Radiative transfer used for cloud remote sensing for decades
- Climate impact of clouds has been main focus
  - how do we represent them in climate models?
  - what are their radiative effects?
- Minimal use for weather and other practical applications
  - recent incorporation of CO_2-slicing cloud heights in NWP models
- Why not more use? Need near real time!
  - cloud property retrievals computer intensive
  - calibrations of visible channels highly uncertain
  - no sales

What's New?

- Computers & networks are now very fast
  - satellite data available nearly anywhere minutes after acquisition
  - complex programs run quickly near-real time possible
  - display of results easy and informative
- Cloud retrievals more mature
  - more confidence in retrievals
  - most operational satellites have necessary channels for more info
- Calibration more reliable
  - self-calibrated MODIS et al. calibrate operational imagers
- Demand
  - modelers see benefits, can use more data now
  - new applications will find users

Aircraft Icing

- Aircraft structures act as ice nuclei in supercooled clouds
    - ice collects, weight increases, plane falls
- Pilots need to know where and when icing can occur
    - PIREPS are first order
        - sparse, aircraft dependent, location uncertain
    - weather forecasts
        - freezing levels, cloud expectations
    - radar => precipitation
- All combined in NCAR/FAA/NOAA/NASA program to provide Current Icing Potential (CIP) & Future Icing Potential (FIP) products to pilots
    - some inadequacies remain
        - NWP uncertainties, intensity, altitude of icing, etc.

Remote Sensing of Icing Conditions

ICING CONDITIONS ARE DETERMINED BY CLOUD

- liquid water content, *LWC* — **positive w/ intensity**
- temperature, *T(z)* — **negative w/ intensity**
- droplet size distribution, *N*(*r*) — ***r* positive w/ intensity**

SATELLITE REMOTE SENSING CAN DETERMINE CLOUD

- optical depth, τ
- effective droplet size, *re*
- liquid water path, *LWP*
- cloud top temperature, *Tc*
- thickness, *h*

IN CERTAIN CIRCUMSTANCES

Radiative Transfer for Operational Remote Sensing

- For operational satellites (e.g., GOES or AVHRR), need means to represent multi-spectral radiance field for full range of expected conditions (surface, atmosphere, cloud)

    - three (four) wavelengths: 0.65, 3.8, 11.0, 12.0 µm

- LaRC approach (based on adding-doubling RTM)

    - compute 0.65 & 3.8 cloud reflectances in black vacuum, create LUTs for range of r_e and D_e, τ over all SZA, VZA, RAA

    - parameterize effective emissivity of clouds at 3.8, 11.0, 12.0 µm

    - create LUT of Rayleigh scattering at 0.65 µm

    - parameterize AD code using LUTs and surface reflectance => **TOA reflectances, R_i**

    - apply simple layer RT for 3.8, 11.0, 12.0 µm using gaseous absorption/emissivity based on correlated k-dist computed using NWP soundings => **TOA brightness temperatures, T_i**

- Find closest match between $R_i(r_e/D_e,\tau,p)$ & $R_i(obs)$; $T_i((r_e/D_e,\tau,p)$ & $T_i(obs)$

Scattering Phase Functions for Clouds Used in LaRC LUTs

0.65 µm 3.75 µm

Ice

Hexagonal columns

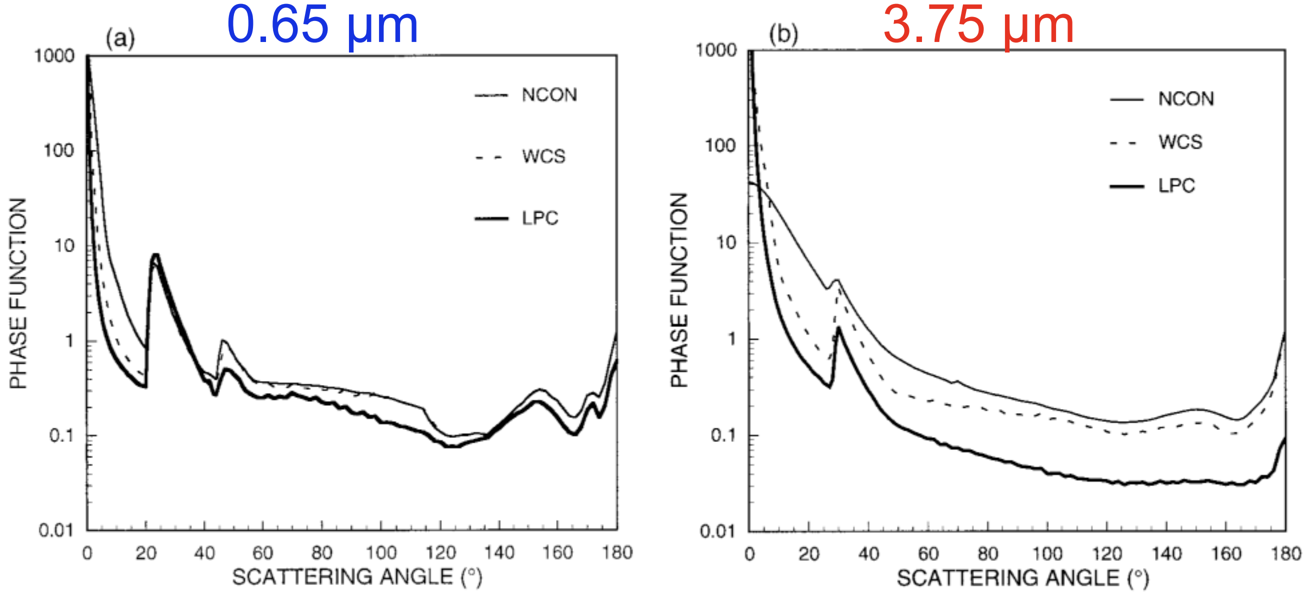

FIG. 3. Scattering phase function for three different ice cloud models (forward scattering maxima have been clipped) for (a) $\lambda = 0.65\ \mu m$ and (b) $\lambda = 3.75\ \mu m$.

Water

Var = 10%

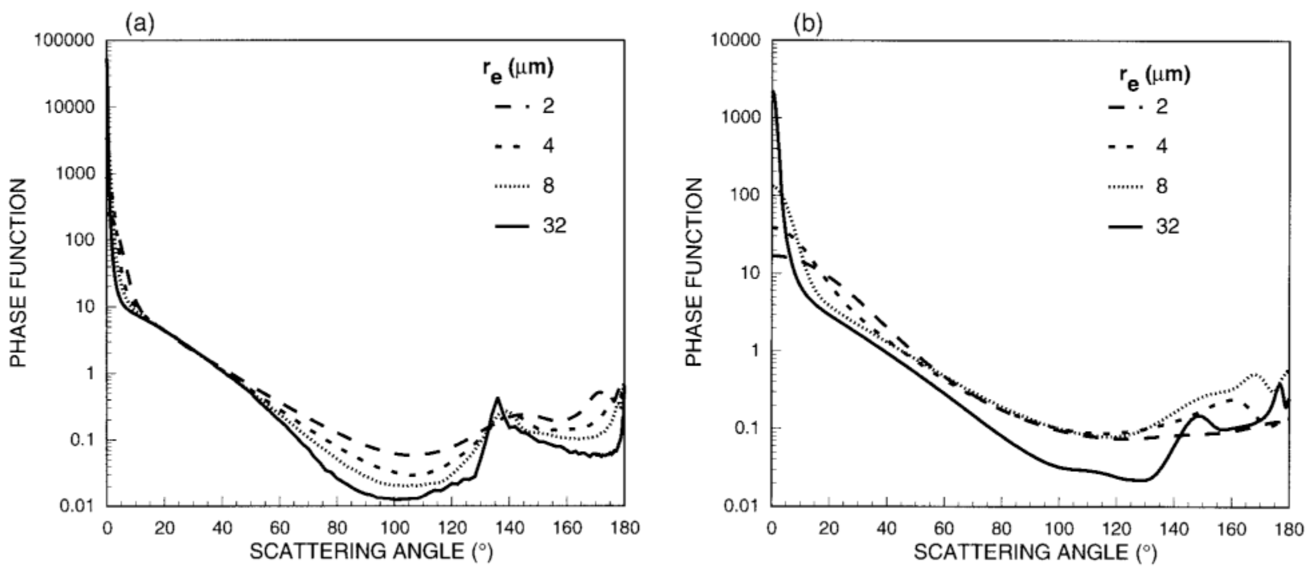

Minnis et al., JAS 98

FIG. 4. Theoretical Mie scattering phase functions for modified gamma distributions of water droplets at (a) $\lambda = 0.65\ \mu m$ and (b) $\lambda = 3.75\ \mu m$.

AD Results for reflectance

0.65 µm

3.75 µm

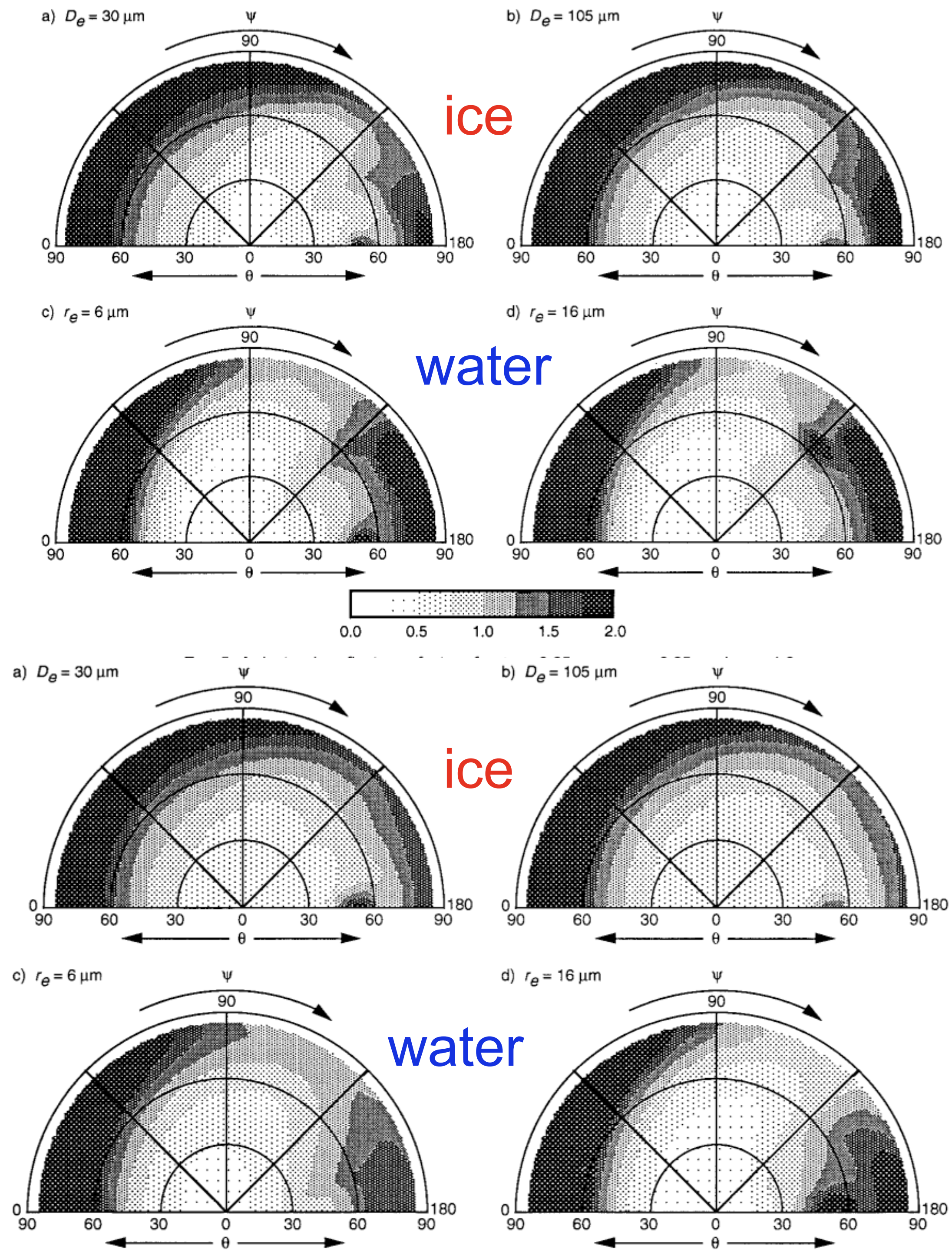

Minnis et al., JAS 98

AD Results for diffuse albedo

0.65 µm

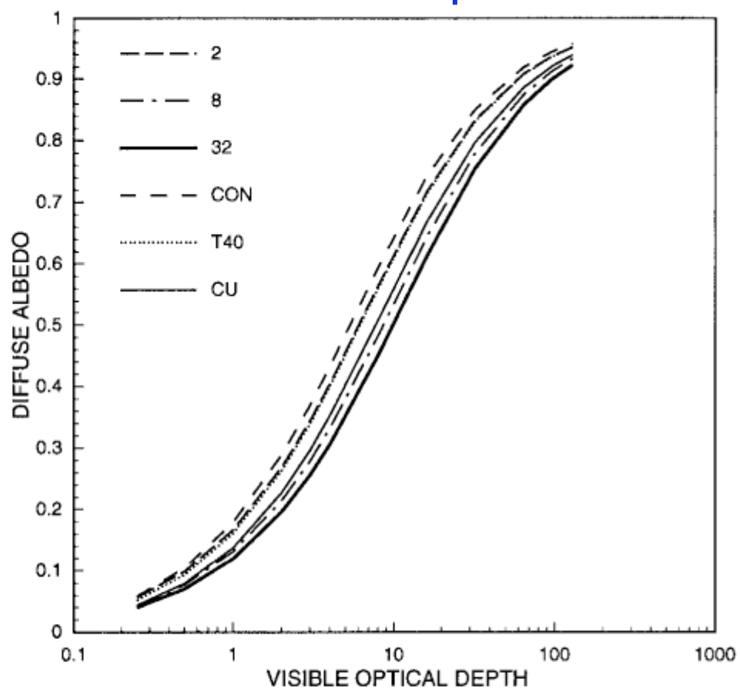

FIG. 9. Diffuse albedos for model clouds at $\lambda = 0.65\ \mu m$.

3.75 µm

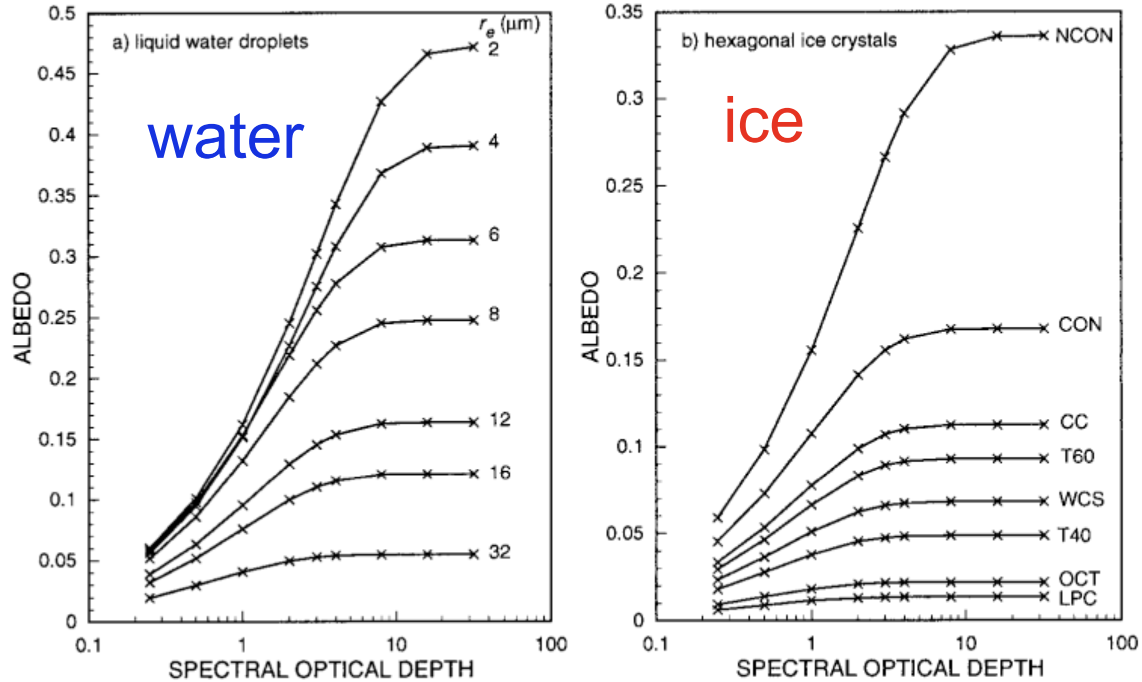

FIG. 10. Diffuse albedo for model clouds at $\lambda = 3.75\ \mu m$. [Note scale differences between (a) and (b).]

Minnis et al., JAS 98

Single-Layer Cloud Reflectance Model

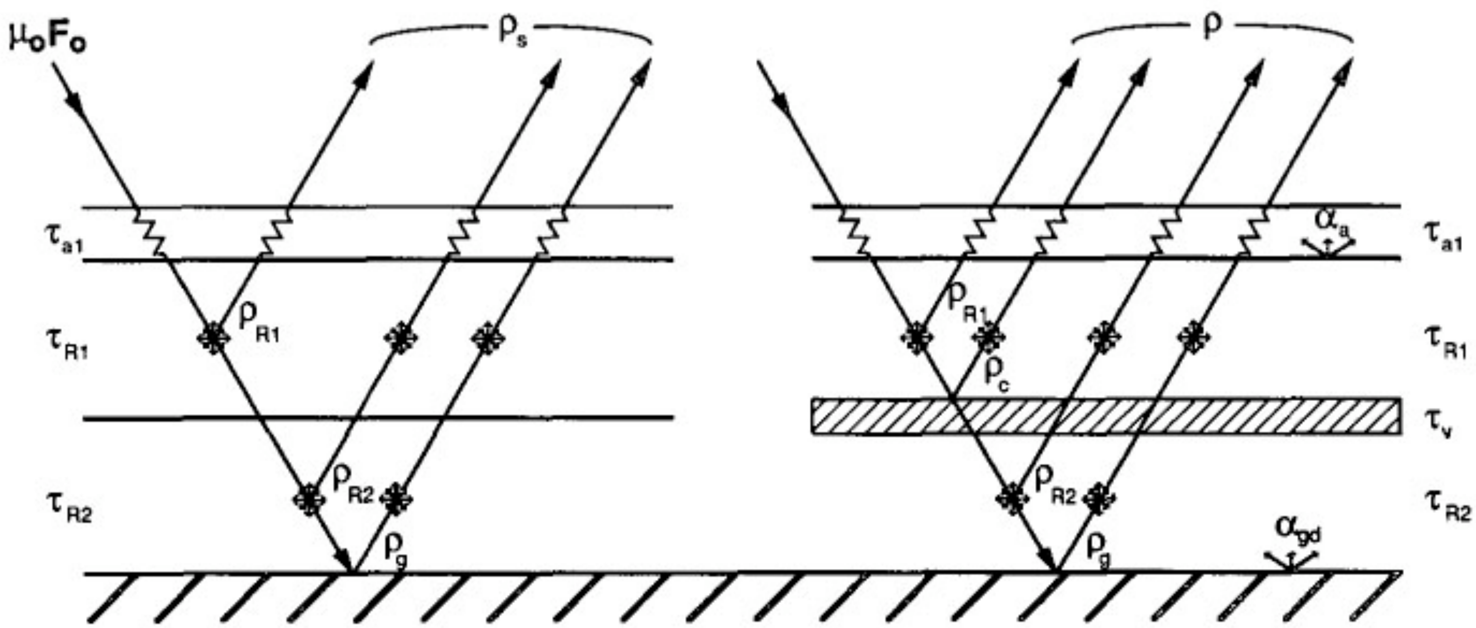

FIG. 3. Schematic diagram of scattering and absorption processes for a three-layer atmosphere with no clouds (left) and with one cloud layer (right).

Visible Parameterization

$$R_{TOA} = (R_{as} + \Delta R)\exp(-\tau_{gas}(1/\mu + 1/\mu_o))$$

AD Lite

$R_{12} = \rho_{R1} + \alpha_c' D_1(1 - \alpha_{Rd1}) + t_{R1}(\mu)[t_{R1}(\mu_o)\rho_c + S_1]$ (1)

where

$\alpha_c' = \alpha_c t_{R1}(\mu_o) + [1 - t_{R1}(\mu_o)]\alpha_{cd}$,
$D_1 = T_1(1 + S_1)$,
$S_1 = \alpha_{Rd1}\alpha_{cd} / (1 - \alpha_{Rd1}\alpha_{cd})$,
$T_1 = 1 - t_{R1}(\mu_o) - \alpha_{R1}$,
$\mu, \mu_o = \cos\theta, \cos\theta_o$,

t_R is the direct Rayleigh transmission as defined by Minnis et al. (1993), and the numeric indices refer to a layer or combination of layers. The downward transmittance of the two layers is

$$T_{12} = D_1[T_2 + t_c(\mu)] + T_2 t_{R1}(\mu_o),$$

where

$T_2 = 1 - \alpha_c' - t_c(\mu_o)$

and t_c is the direct transmittance of the cloud (Minnis et al. 1993).

The combined reflectance for the three layers is

$$R_{123} = R_{12} + \alpha_{Rd2} D_2 T_{12}^* + (\rho_{R2} t_c(\mu_o) t_{R1}(\mu_o) + S_2) t_c(\mu) t_{R1}(\mu),$$

where

$D_2 = T_{12}(1 + S_2)$,
$S_2 = Q_2 / (1 - Q_2)$,
$Q_2 = \alpha_{Rd2} R_{12}'$,
$R_{12}' = \alpha_{R1} + (1 - \alpha_{Rd1}) D_1 \alpha_{cd} + t_{R1}(\mu)[\alpha_{cd} t_{R1}(\mu_o) + S_1)$
$T_{12}^* = U_1^*(1 - \alpha_{Rd1})$,

and

$U_1^* = (1 - \alpha_{cd})(1 + S_1)$.

The downward transmittance for the three layers is

$$T_{123} = D_2[T_3 + t_c(\mu)] + T_2 t_{R1}(\mu_o),$$

where

$$T_3 = 1 - \alpha_{Rd2} - t_{R2}(\mu_o).$$

The combined atmosphere and surface reflectance is

$$\boxed{R_{as} = R_{123} + \alpha_{sd} T_{123}^* D_3 + t_{123}(\mu)[\rho_s t_{123}(\mu_o) + S_3], \quad (2)}$$

where α_{sd} and ρ_s are the diffuse surface albedo and surface bidirectional reflectance, respectively,

$t_{123}(\mu) = t_{R1}(\mu) t_c(\mu) t_{R3}(\mu)$
$t_{123}(\mu_o) = t_{R1}(\mu_o) t_c(\mu_o) t_{R3}(\mu_o)$
$D_3 = T_{123}(1 + S_3)$,
$S_3 = Q_3 / (1 - Q_3)$
$Q_3 = \alpha_{sd} R_{123}'$,
$T_{123}^* = T_{12}^* U_2^*$,
$U_2^* = (1 + S_2^*)(1 - \alpha_{Rd2})$,
$S_2^* = R_{12}^* \alpha_{Rd2} / (1 - R_{12}^* \alpha_{Rd2})$,
$R_{12}^* = \alpha_{cd} + U_1^* \alpha_{Rd1}(1 - \alpha_{cd})$,

and

$R_{123}' = R_{12}' + \alpha_{Rd2} D_2 T_{12}^* + [S_2 + \alpha_{R2} t_c(\mu_o) t_{R1}(\mu_o)] t_{R1}(\mu) t_c(\mu)$.

Values for α_{sd} and ρ_s are estimated from the estimated clear-sky diffuse albedo α_{csd} (Minnis et al. 1993) and the observed clear-sky reflectance, ρ_{cs}.

$$\alpha_{sd} = 1.149\,\alpha_{csd} - 0.0333. \qquad (3)$$

$$\rho_s = \rho_s' - D\,\alpha_{sd} / \exp(-\tau_{R13}/\mu_o), \qquad (4)$$

where

$\rho_s' = [\rho_{cs} / \exp(-\tau_{gas}(1/\mu + 1/\mu_o)) - \rho_{R13}] / (1 - \alpha_{Rd13})$
$D = (1 + S)(1 - \alpha_{R13} - \exp(-\tau_{R13}/\mu_o) + S\exp(-\tau_{R13}/\mu_o)$,
$S = \alpha_{sd}\alpha_{Rd13} / (1 - \alpha_{sd}\alpha_{Rd13})$,

and

τ_{gas} is the absorption optical depth for the gaseous absorbers, such as ozone and water vapor, for the

$$\boxed{\Delta R = a_o + \sum_{i=1}^{3} a_i \mu_o^{\,i} + \sum_{i=1}^{3} b_i \mu^i + \sum_{i=1}^{6} c_i \Theta^i}$$

Parameterization errors

Table 1. Relative differences in TOA reflectance between parameterization and AD calculations.

α_{sd} (%)	new parameterization	old parameterization
4-10	-0.01 ± 0.53 %	-0.08 ± 5.1 %
10 -50	-0.01 ± 0.67 %	-0.14 ± 7.0 %
50-90	0.03 ± 1.04 %	-4.3 ± 12.4 %

Minnis et al., TGARS 08

Parameterization of Brightness Temperatures

Example of AD results, ε

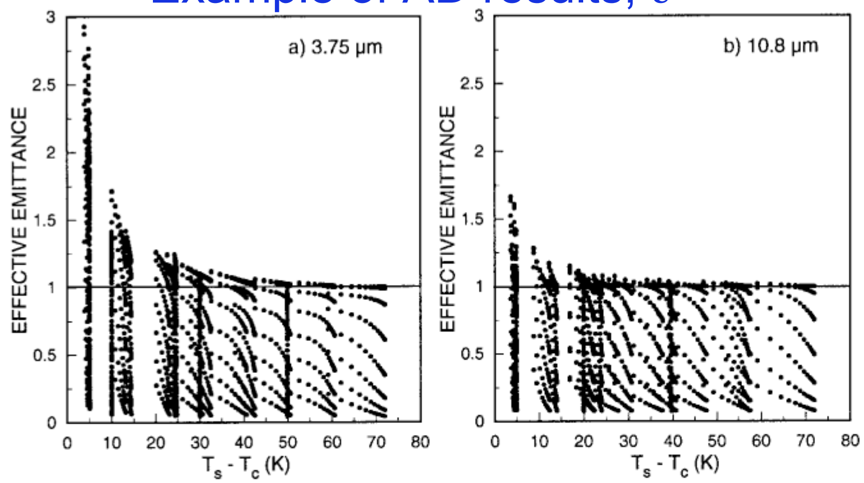

FIG. 12. Variation of effective emittance with clear-cloud temperature difference from adding–doubling model calculations for $r_e = 6\ \mu$m.

Radiance at cloud top

$$B_\lambda(T_\lambda) = \varepsilon_\lambda B(T_c) + (1 - \varepsilon_\lambda)B(T_b) + \rho_\lambda \mu_0 E_\lambda \delta(d),$$

Parameterization of ε

$$\varepsilon(\zeta, \mu, \xi) = \sum_{i=0}^{2} \sum_{j=0}^{4} \sum_{k=0}^{1} d_{ijk}\zeta^i \mu^j \xi^k,$$

$\zeta = 1/\ln(\Delta T_{sc})$

$\mu = \cos$ VZA

$\xi = 1/\ln(T_s)$

Parameterization errors

TABLE 10. Rms temperature differences between AD model and emittance parameterization.

Model	3.75-μm ΔT (K) All	3.75-μm ΔT (K) $\epsilon < 1$	3.90-μm ΔT (K) All	3.90-μm ΔT (K) $\epsilon < 1$
		Water		
r_e (μm) =				
2	1.16	0.71	1.07	0.67
4	1.21	0.69	1.16	0.69
6	1.02	0.55	1.00	0.57
8	0.81	0.48	0.81	0.48
12	0.55	0.36	0.55	0.37
16	0.42	0.30	0.42	0.30
32	0.22	0.18	0.22	0.18
		Ice		
NCON	2.44	1.13	2.20	0.84
CON	1.62	1.04	1.45	0.90
CC	1.22	0.75	1.04	0.64
T60	1.06	0.62	0.90	0.56
CS	0.92	0.54	0.81	0.42
WCS	0.83	0.44	0.70	0.37
T40	0.63	0.32	0.52	0.27
NOV	0.45	0.26	0.38	0.19
OCT	0.32	0.17	0.25	0.13
CU	0.27	0.15	0.21	0.11
LPC	0.21	0.12	0.16	0.09

Minnis et al., JAS 98

Brightness Temperature Differences from Parameterization

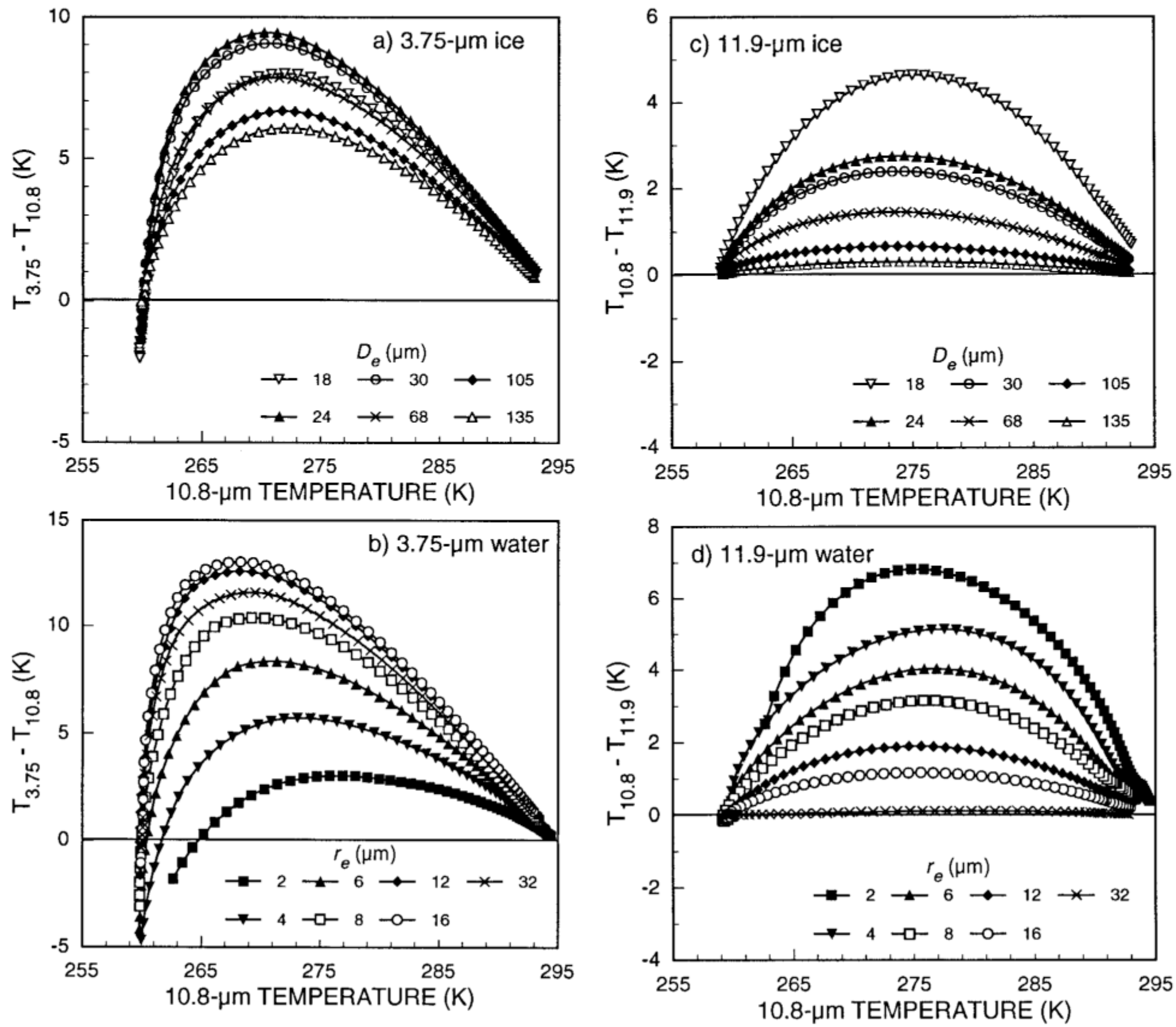

FIG. 14. Brightness temperature differences from parameterizations for $T_s = 295$ K, $T_c = 260$ K, $\tau < 16$, and $\theta = 30°$.

Minnis et al., JAS 98

Finding a Solution, Given

$R_i(obs)$, $T_i(obs)$

Try to compute solutions iteratively for (A) ice and (B) water, if T(11) > 233 K.

Use logic to deduce phase

- no retrieval
- Teff
- smallest error
- agreement w/T11-T12

In most cases, no retrieval or Teff decides phase!

Visible Infrared Solar-infrared Split-window Technique **(VISST)**

Minnis et al., NASA 95

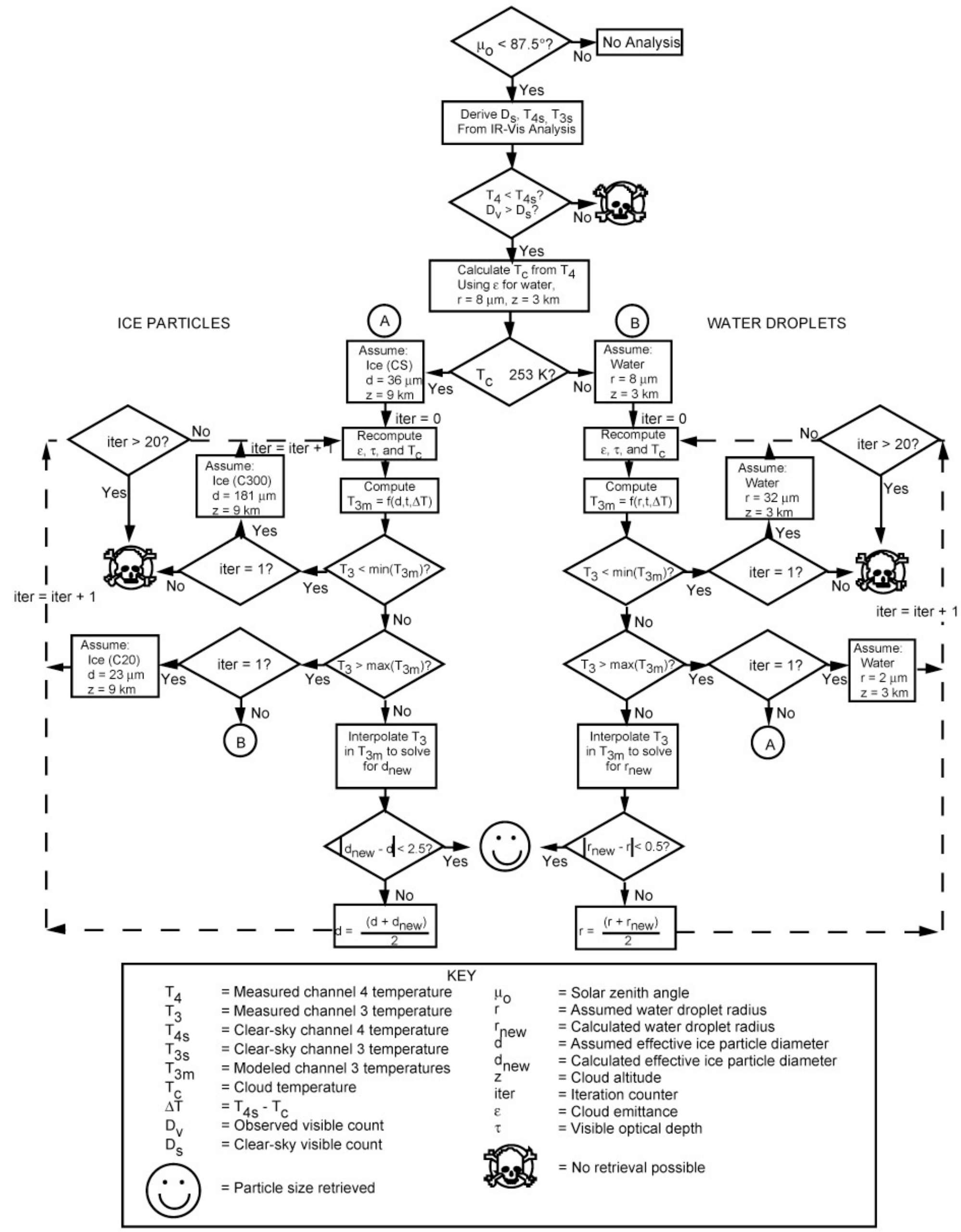

Figure 4.3-10. Flow diagram of channels 1, 3, and 4 cloud property retrieval algorithm. Effective diameter is denoted with *d*; effective radius is *r*.

Putting Parameterizations into Near-Real-Time Operation for GOES

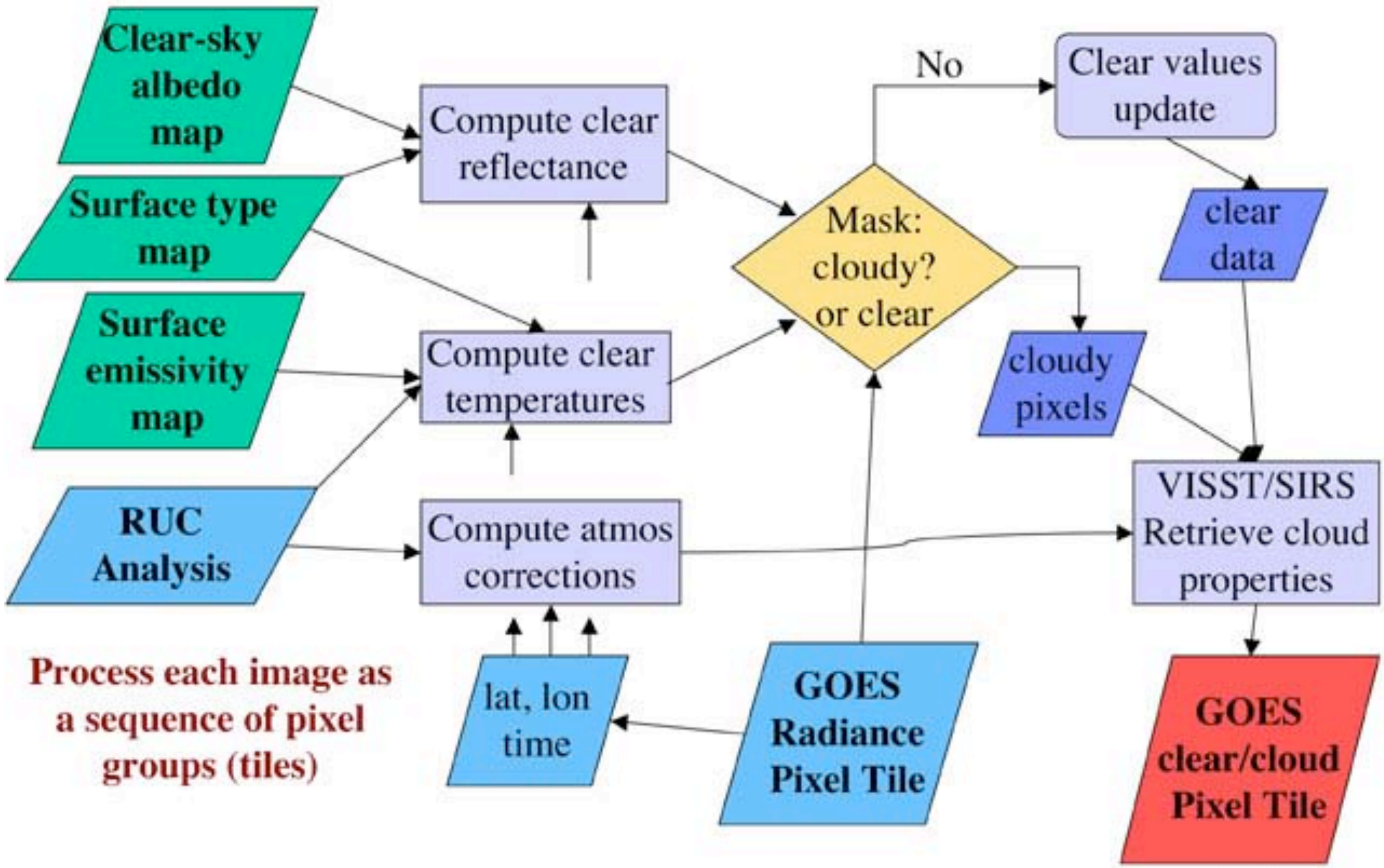

Products Derived from Geostationary & Polar-Orbiting Satellites

Current Products

0.65 μm Reflectance	3.7 μm Temperature	6.7 μm Temperature
10.8 μm Temperature	12 or 13.3-μm Temp	1.6 μm Reflectance
Skin Temperature	Optical Depth	Eff Radius/Diameter
Liq/Ice Water Path	Cloud Eff Temp	Cloud Top Pressure
Cloud Eff Pressure	Cloud Top Height	Cloud Eff Height
Cloud Phase	Cloud Bot Height	Cloud Mask
Cloud Bot Pressure	Icing Potential	Broadband SW Albedo
Broadband LW Flux	Infrared Emittance	

New products:

Surface Flux (Gridded)

Multi Layer Cloud Mask & Layer Retrievals

http://www-angler.larc.nasa.gov/satimage/products.html

Analysis Applied to Two Satellites to Cover USA

1645 UTC, 4 Dec 2007

GOES-11 RGB

GOES-12 RGB

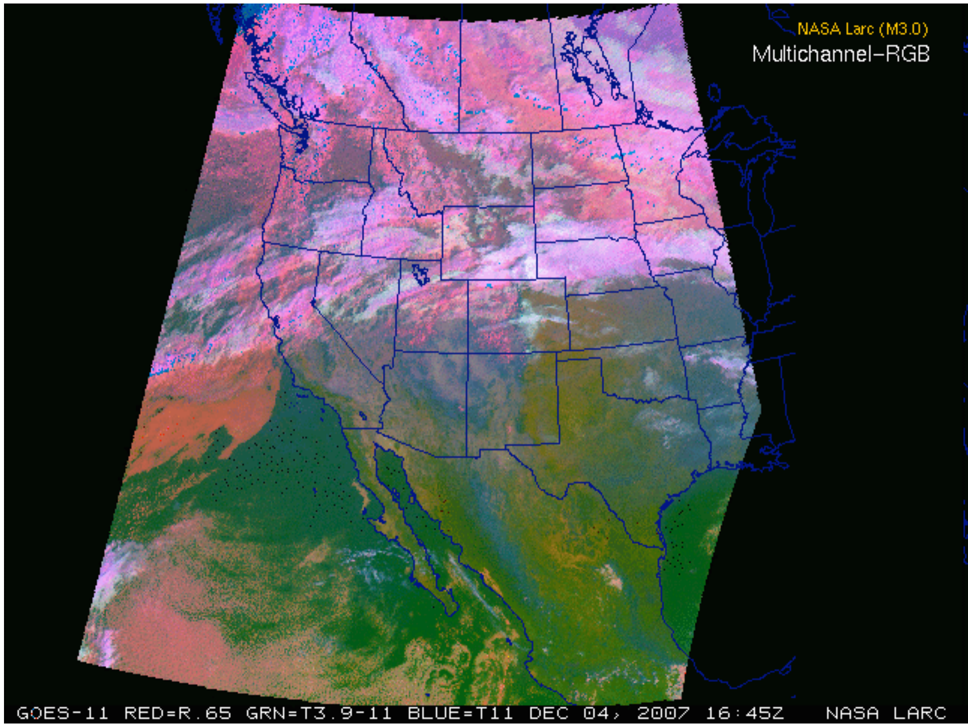

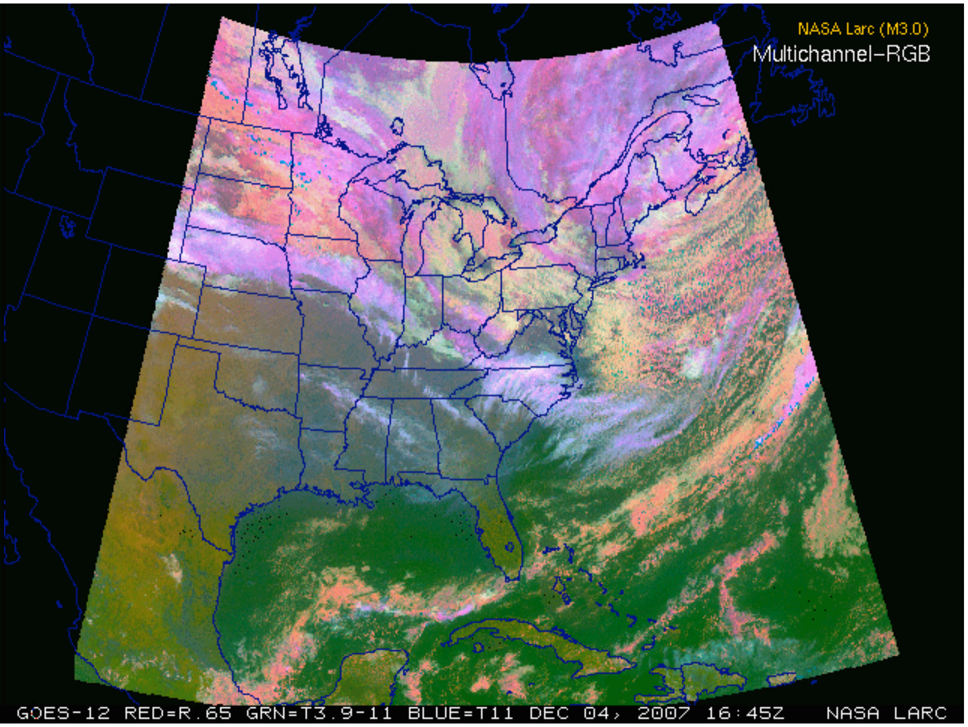

Each image is analyzed and the results are combined

Combined GOES-11/12 Retrievals, 1645 UTC 4 Dec 2007

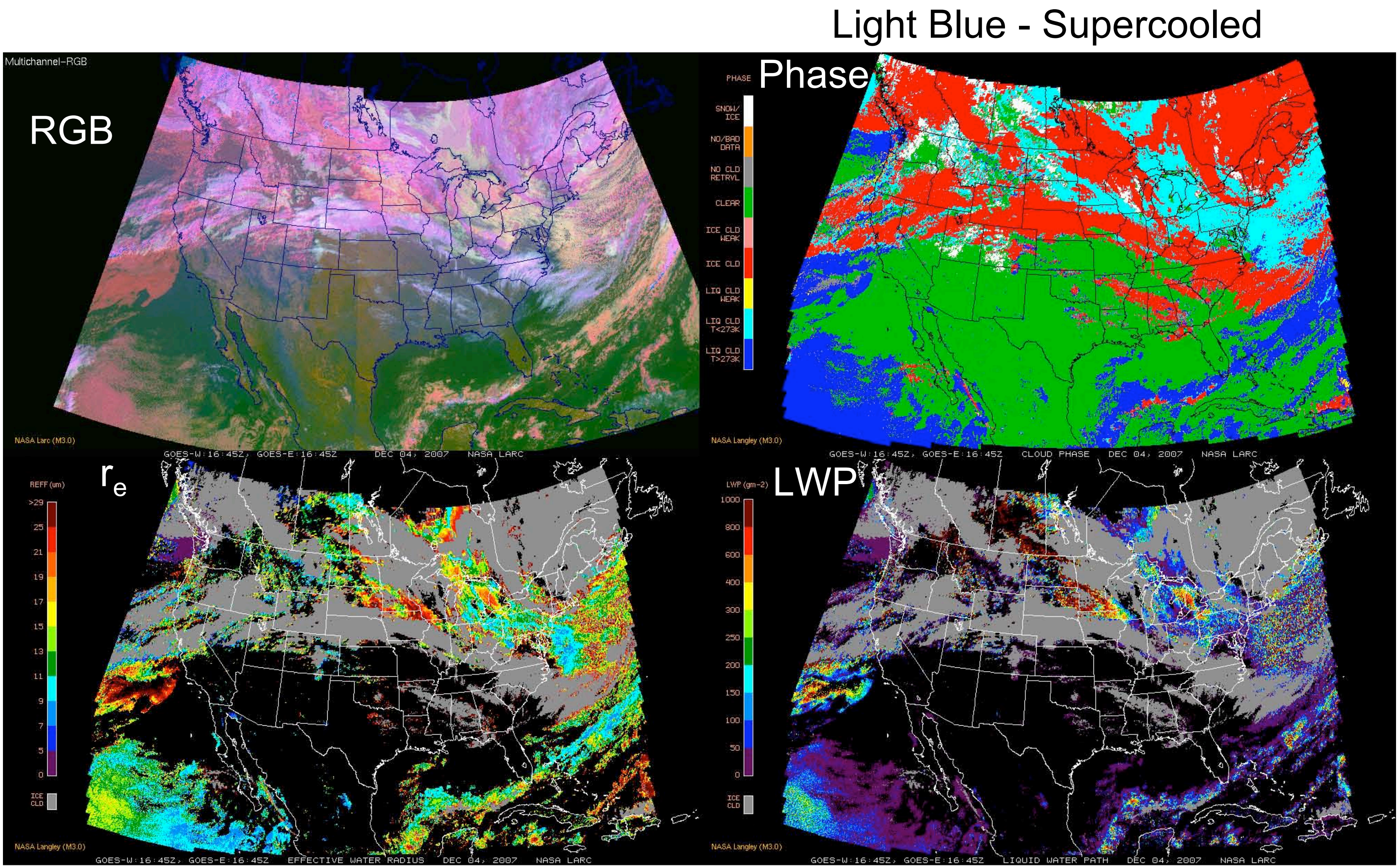

CLOUD PRODUCTS VS. ICING PARAMETERS

- $LWP = LWC * h$

- $re = \mathrm{f}[N(r)]$

- **Tc & h can yield depth of freezing layer**

- **z_t is top of icing layer**

- **ceiling = z_t - h**

IN MANY CASES, SATELLITE REMOTE SENSING
SHOULD PROVIDE ICING INFORMATION

GOES SLW vs. PIREPS Icing

Compared to Positive icing PIREPS and provided there were no overcast ice clouds, LaRC GOES technique detected SLW 98% of the time (Smith et al., 2000)

Comparison of GOES Cloud Properties with PIREPS Icing Intensity
N=7800 (Jan-March, 2003)

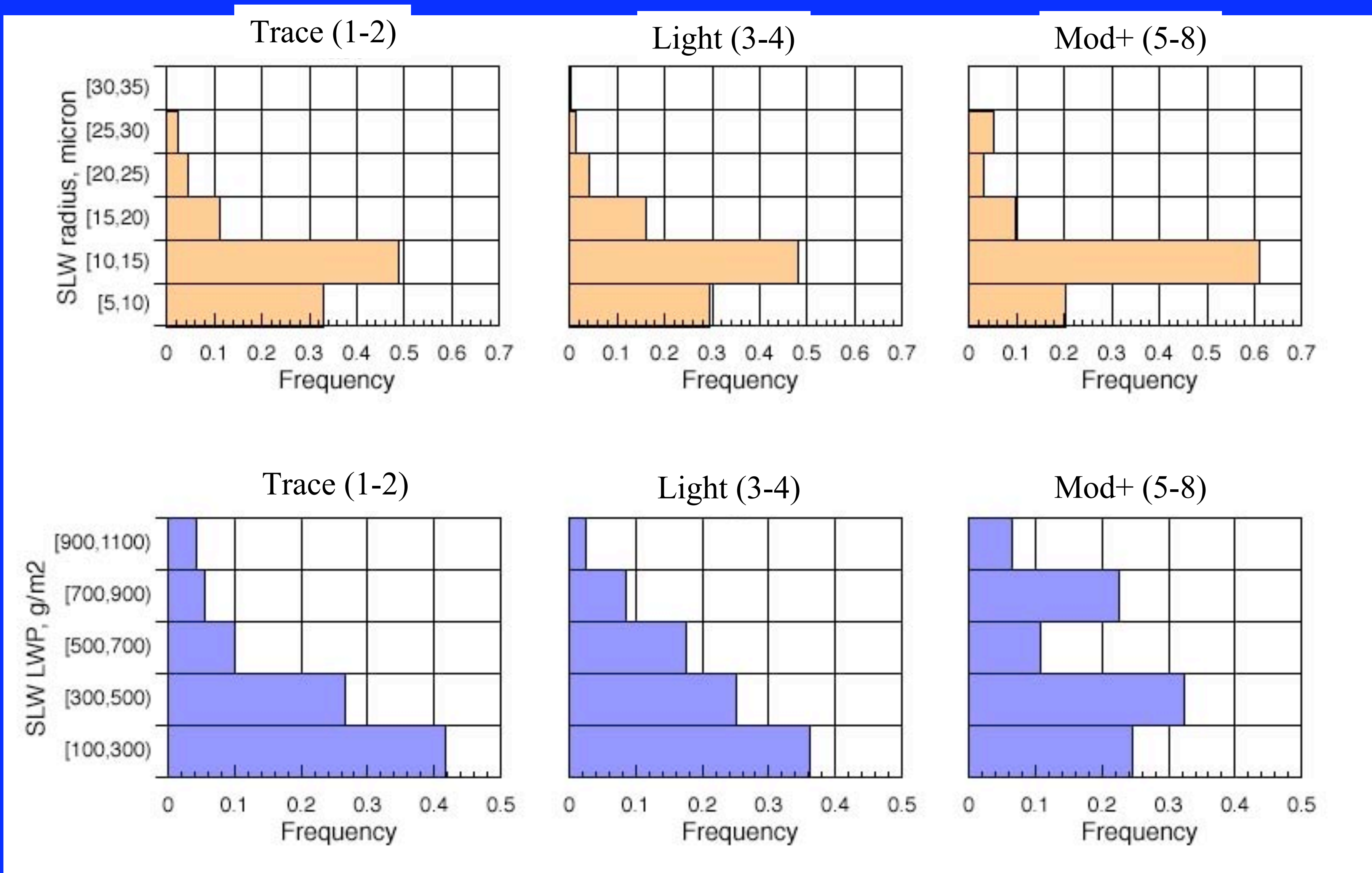

Comparison of LWP with 18,000 PIREPS, 5 Jan -5 Apr, 2005

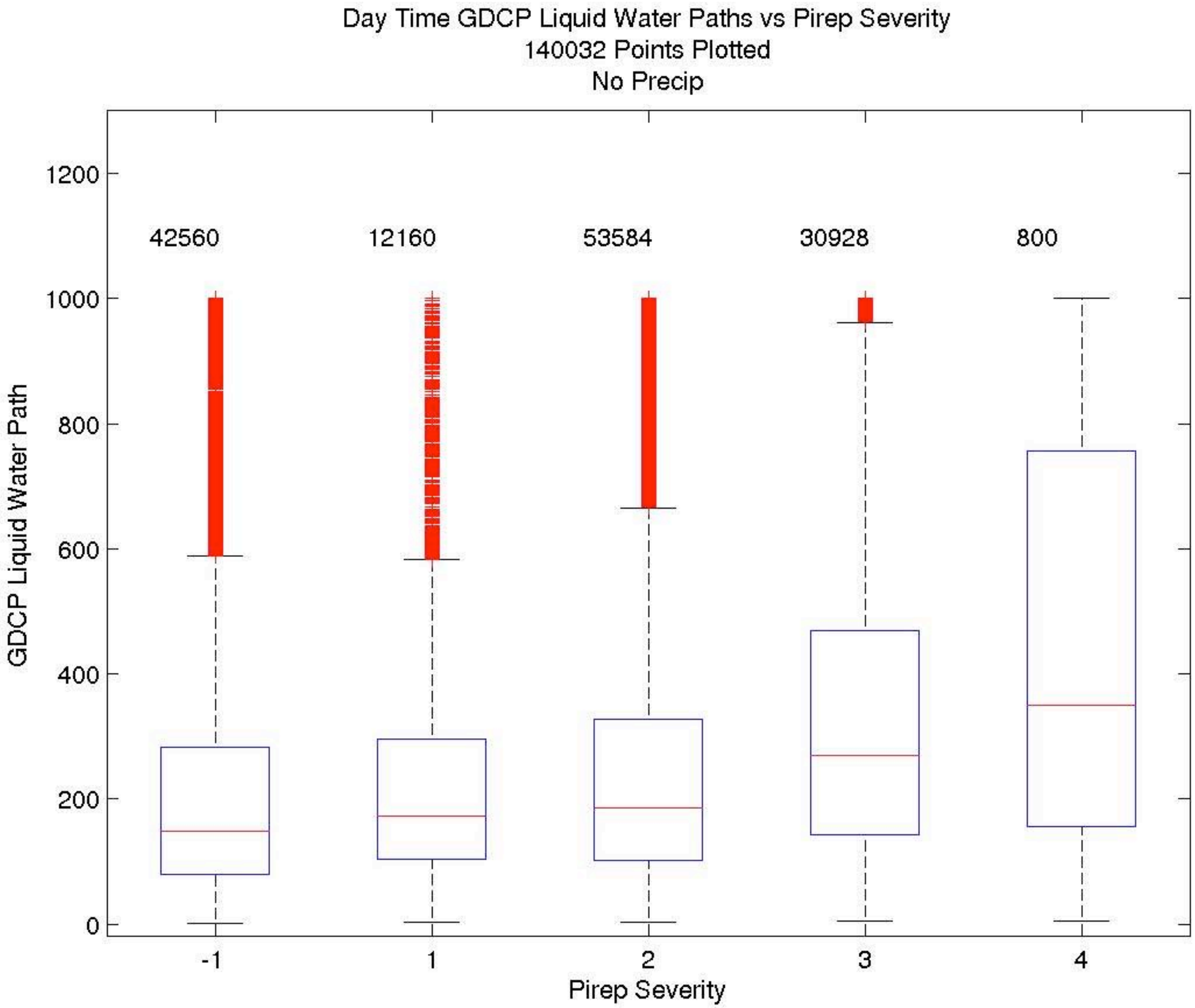

Haggerty et al., JCAM 08

Dependence of Icing on LWP and r_e

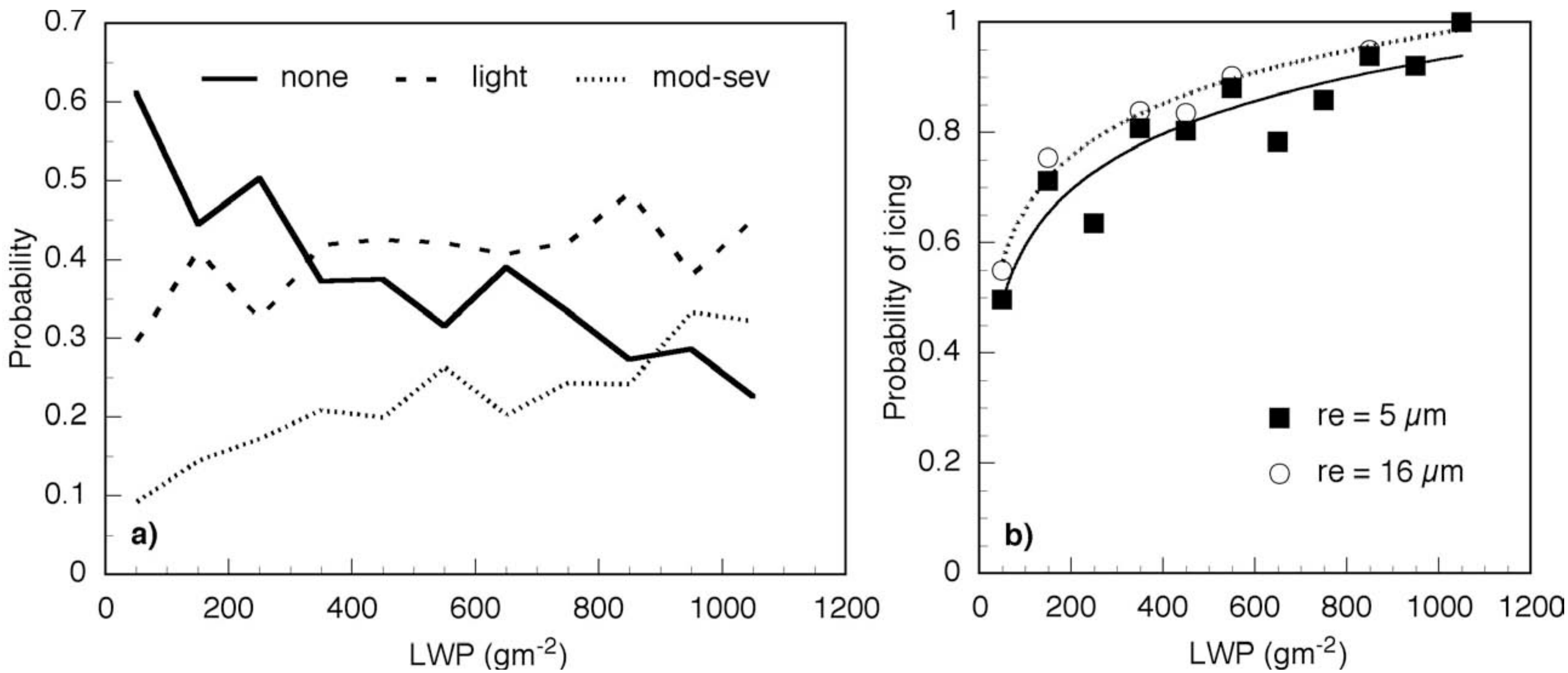

Major dependence on LWP, minor on r_e

Formulation developed for icing potential

Icing Potential from GOES Data Alone

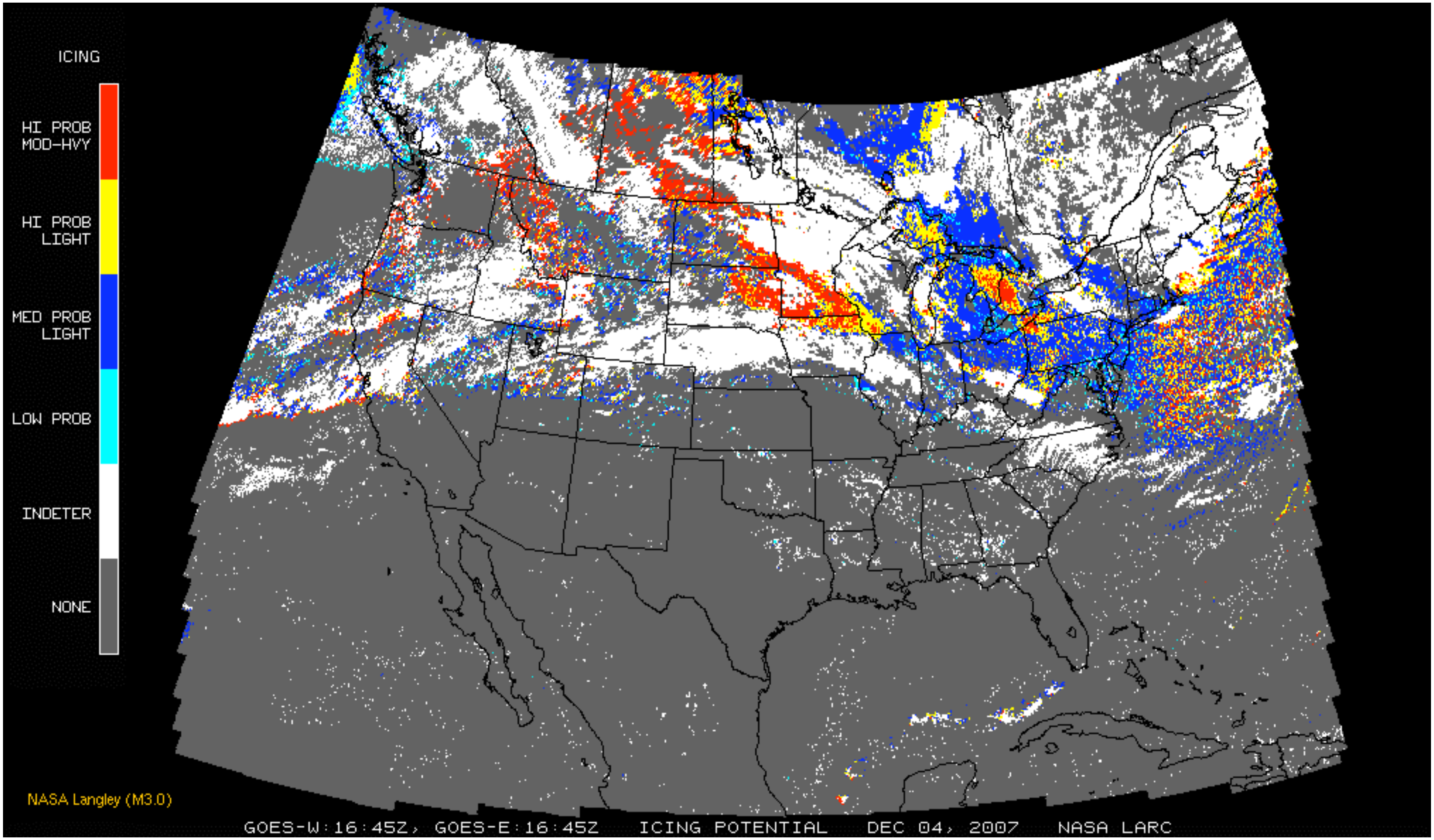

Many indeterminate areas (white)

Integration of Cloud Products into NCAR CIP

16 UTC 16 Feb 2005

GOES Cloud Properties

CIP Icing Severity Product

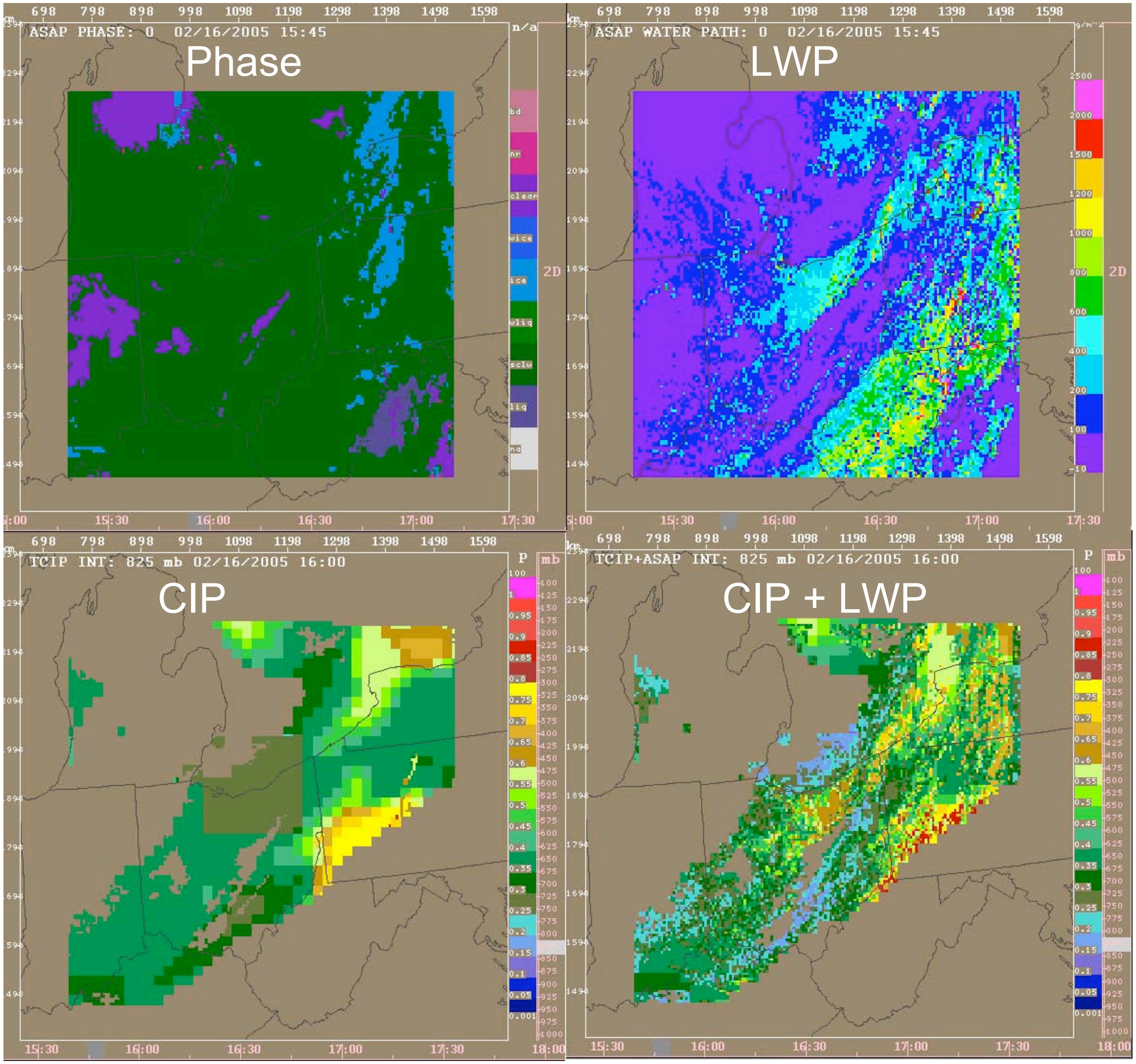

Haggerty et al., JCAM 08

Finding More Icing in Indeterminate Areas

Multilayer Cloud Detection & Retrieval

- Some indeterminate cloudy pixels are overlapped ice over water clouds
  - multilayered cloud detection needed to find those areas where icing is a problem
- Need a multilayered VISST to derive low cloud properties

Use AD model to develop LUTs for ice over water clouds

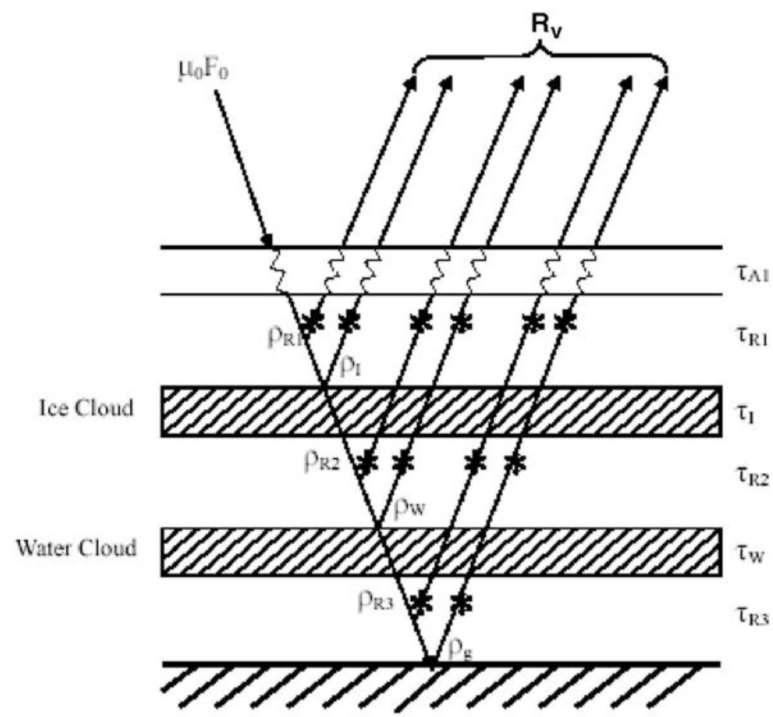

Minnis et al. JGR 2007

Multilayered Cloud Reflectance Fields from AD Computations

Total WP - 200 gm^{-2}, Vary LWP

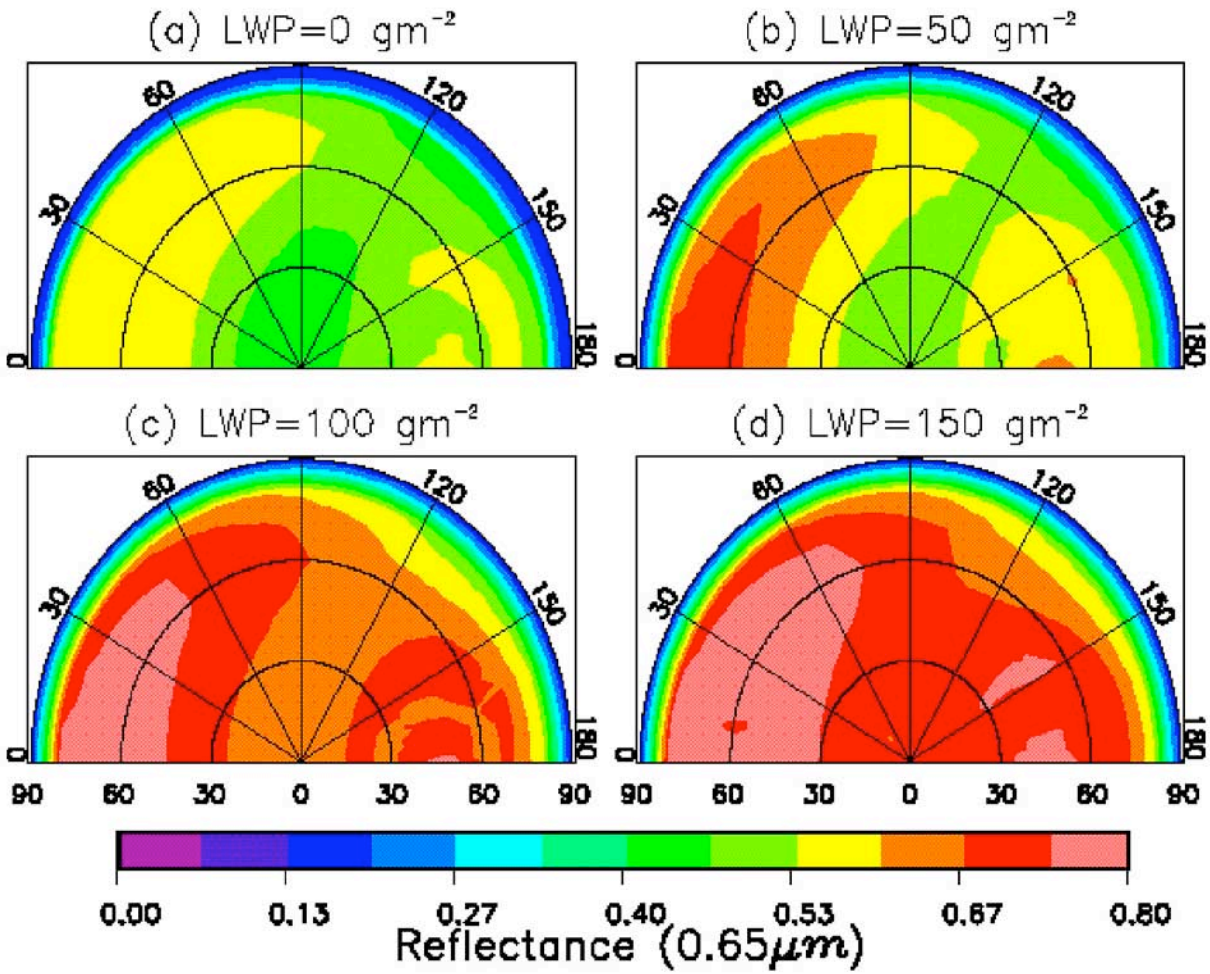

BRDF varies dramatically as mix of ice and water changes

Minnis et al. JGR 2007

Multi-layered Cloud Detection, 13.3/10.8 μm

1645 UTC 4 Dec 2007

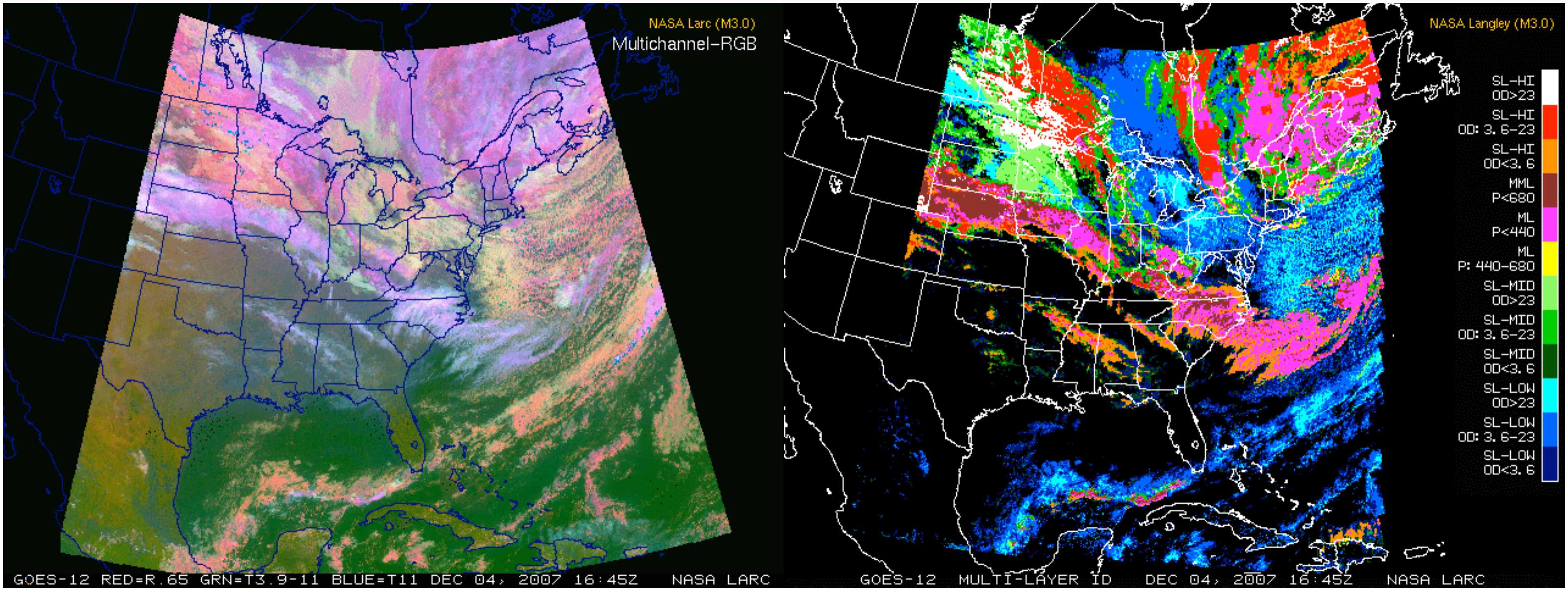

Magenta areas are identified as multilayer ice-over-water

Based on simplification of Chang & Li, JGR 2000 method

Multi-layered Low Cloud Retrieval, ML VISST

1645 UTC 4 Dec 2007

Teff, ML Low

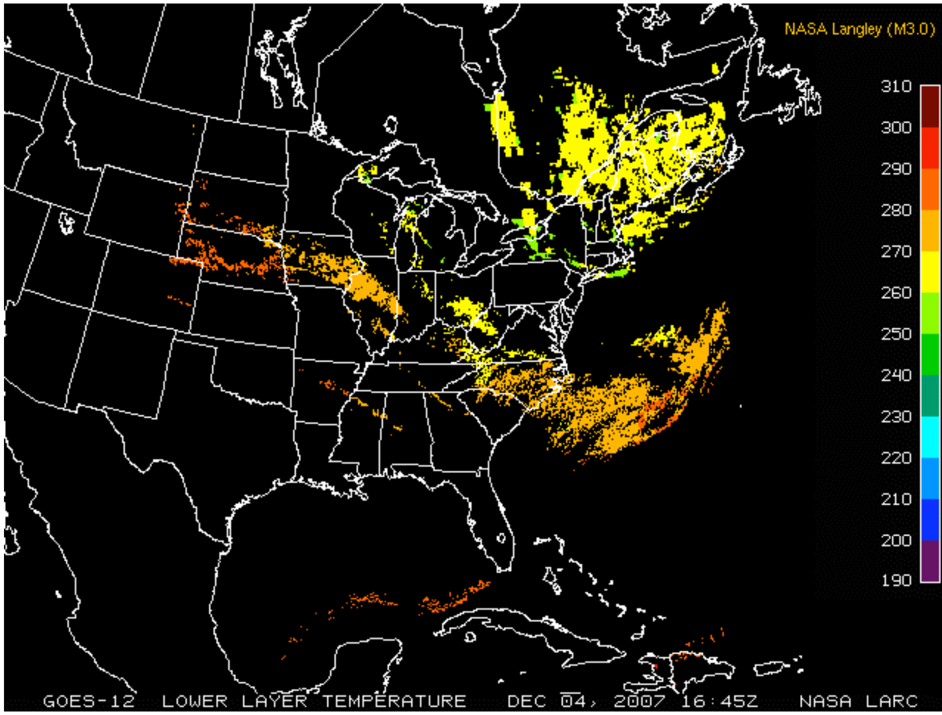

Optical Depth, ML Low

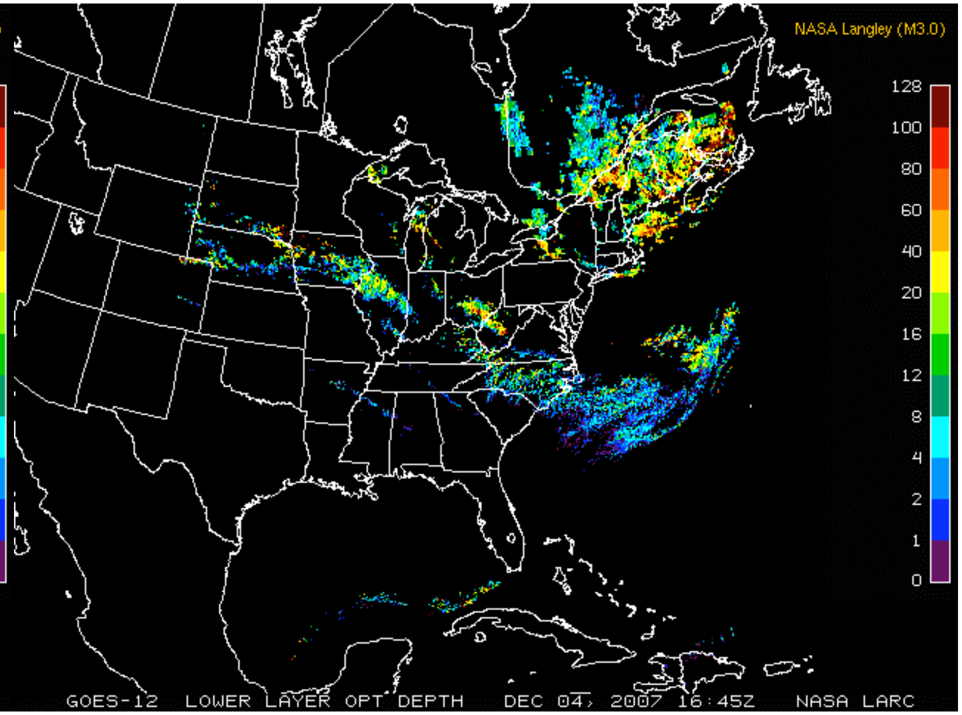

Some retrieved clouds are supercooled

Icing Potential

1645 UTC 4 Dec 2007

Standard retrievals   Standard retrievals + ML results

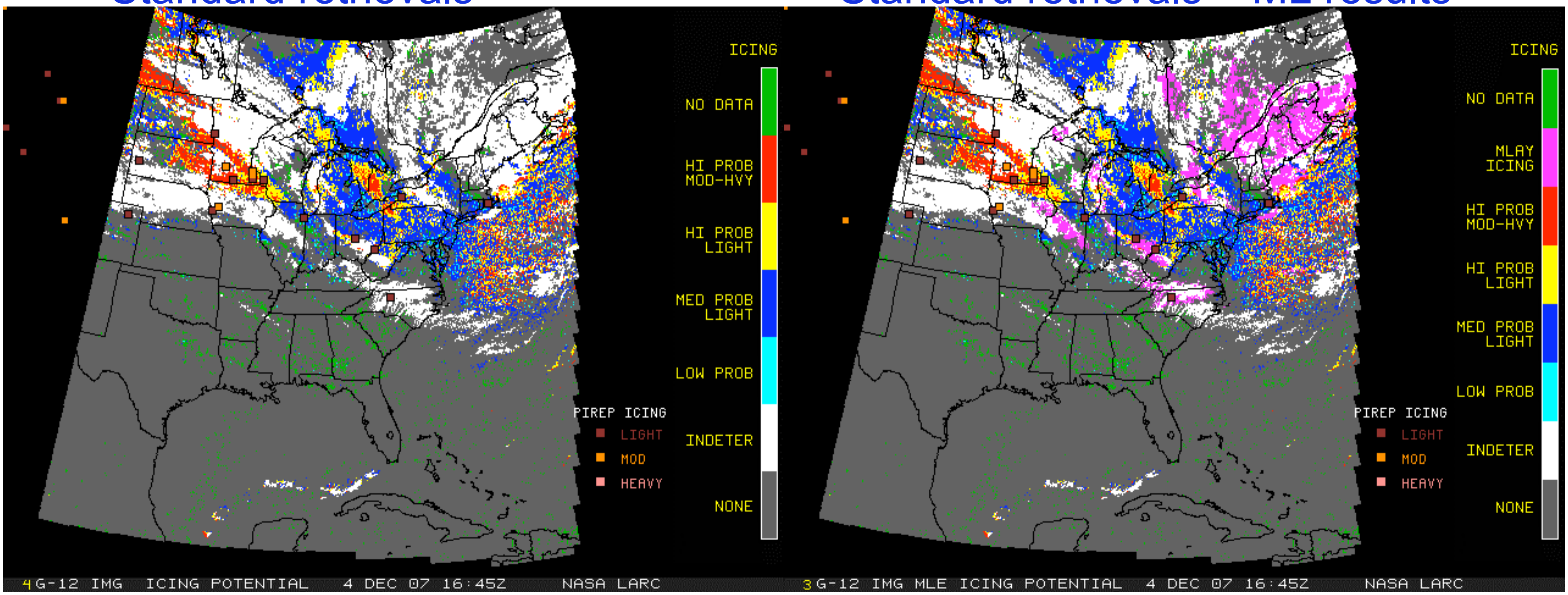

Multilayer retrievals pick up additional areas
with icing that were formerly indeterminate

… some areas remain undetected

When upper cloud is too thick, CO_2 Does Not Help

…may need microwave data

Microwave radiative transfer can be used to determine cloud LWP and temperature of water clouds even when thick ice cloud is present

Temperature derived from TMI MW 37 GHz on TRMM, 1998 for single-layer ice cloud = SST

T_c derived from VIRS imager using VISST

Water cloud temperature derived from TMI MW 37 GHz on TRMM, 1998 for single-layer ice cloud

T_c derived from VIRS imager using VISST

Supercooled clouds can be detected using MW data, day & night

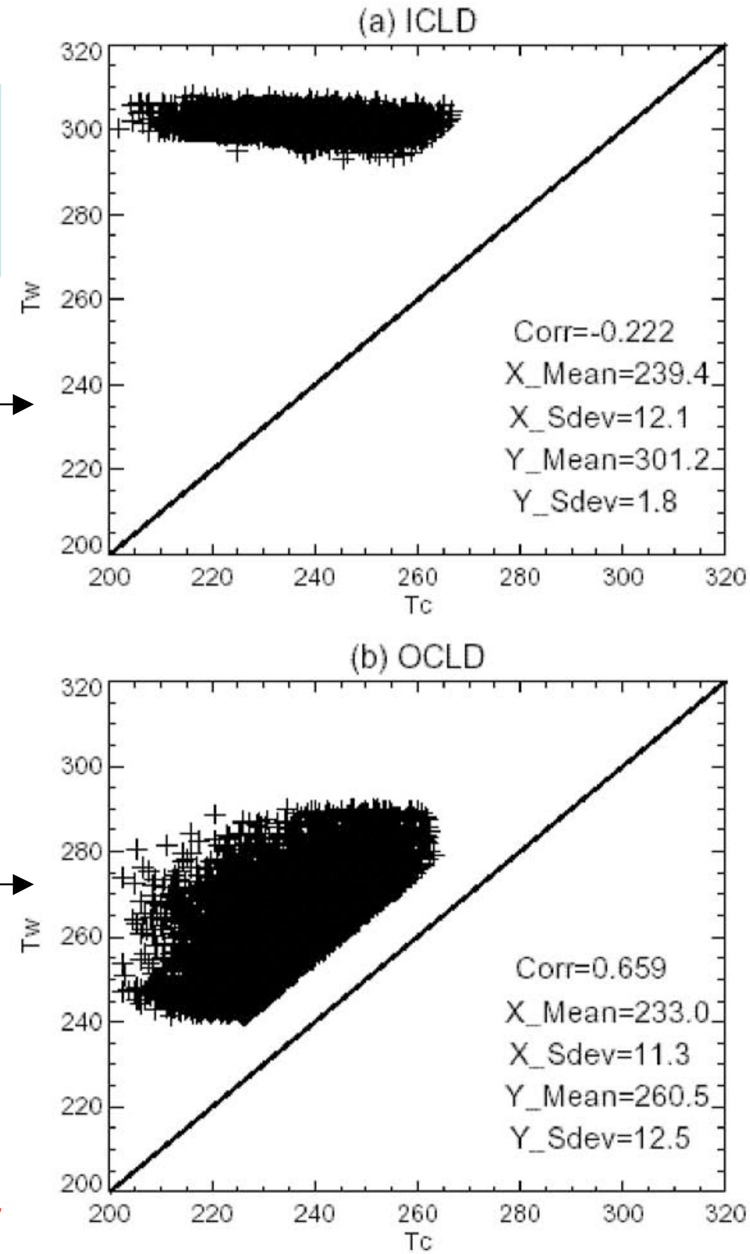

Minnis et al., JGR 2007

Summary & Future Research

- Radiative transfer has enabled the development of new cloud products from real time satellite data
  - application to weather and nowcasting problems
  - proven valuable for aircraft safety products (used in CIP)
  - near-real time cloud properties & radiation budget available over many regions of the globe

- Icing product currently limited to water clouds without overlying cirrus
  - CO_2-slicing with ML VISST looks very encouraging
    - limited to thin cirrus over thick water
  - MW with ML VISST works over ocean
    - need more development over land
    - real time limited because of few polar-orbiters with MW data
      - GEO MW?

- Other applications in process
  - improve icing altitude range more accurately than model
  - cloud products being assimilated into RUC (Ztop, LWP/IWP)
  - potential for ceiling estimation